Electronic structure and stability of the transition metal oxide $Ni_2Ti_4O$



1994 J. Phys.: Condens. Matter 6 2861

(http://iopscience.iop.org/0953-8984/6/15/009)

J. Phys.: Condens. Matter 6 (1994) 2861–2868. Printed in the UK

# Electronic structure and stability of the transition metal oxide $Ni_2Ti_4O$

D Nguyen Manh†§, A Pasturel†, A T Paxton‡ and M van Schilfgaarde‡

† Laboratoire de Thermodynamique et de Physico-Chimie Métallurgiques, Unité de Recherche associée au CNRS 29, Ecole Nationale Supérieure d'Electrochimie et d'Electrométallurgie de Grenoble, BP 75, 38402 Saint Martin d'Hères Cédex, France

‡ SRI International, 333 Ravenswood Avenue, Menlo Park, CA 94025, USA

Received 22 October 1993, in final form 21 January 1994

**Abstract.** The electronic structure of $Ni_2Ti_4O$ is studied using first-principles calculations based on the linear-muffin-tin-orbital method. The role of oxygen in stabilizing the metallic $NiTi_2$-type structure is analysed by site-projected energy calculations which indicate that the Ti(f) sites with non-icosahedral symmetry determine the structural stability of $Ni_2Ti_4O$. The origin of this behaviour, contrary to that found for $NiTi_2$, is due to the effects of 2p(O)–3d(Ti(f)) hybridization.

## 1. Introduction

The transition-metal–transition-metal (TM–TM) compounds of the form TM–$TM_2$ form one of the most interesting classes of intermetallic compounds. For this composition, both geometrically and topologically close-packed structures may occur, emphasizing the different roles played by electronic effects and atomic-size effects in explaining the structural stability of such structures [1]. Among topologically close-packed structures, the $NiTi_2$-type structure displays a peculiar behaviour since it is only partially tetrahedrally packed. Recently [3, 4], we have investigated the electronic structure and the cohesive properties of the $NiTi_2$-related compounds by means of first-principles (FP) calculations. The stability of this structure has been studied as a function of the number of valence electrons and it has been found to be more stable than the $MoPt_2$-type and $MoSi_2$-type structures for electron-to-atom ratios between 4 and 6.5. It has been suggested that this structure is typical of a family of electron compounds. Moreover, a site-projected energy analysis allows us to show that the Ti site with icosahedral symmetry is the favoured site for stabilization in the $NiTi_2$-type structure. On the basis of our previous study, the purpose of this paper is to study the electronic structure and the stability of $Ni_2Ti_4O$ from a microscopic point of view. The interest in $Ni_2Ti_4O$ is that it is reported to display the same large FCC structure as $NiTi_2$ [4]. However, the role of oxygen in the stabilization of the $NiTi_2$-type structure is not well understood. In the phenomenological model proposed by Nevitt [2] for the ternary Ti–TM–O system, it is supposed that O acts with a 'negative valence', i.e. as an electron acceptor, and that the number of 'valency electrons' per TM atom decreases with increasing atomic number for the sequence Mn to Ni. From these assumptions, the stability of the oxide phase can be explained from a rigid-band approximation of the corresponding TM-$Ti_2$ compound for which O, entering interstitial sites as an electron acceptor, reduces

§ Permanent address: Department of Physics, Polytechnic University of Hanoi, Vietnam.

0953-8984/94/152861+08$19.50  

the number of occupied electronic states in the conduction band to a favourable value of the electron-to-atom ratio.

In order to clarify the situation, we decide to study the stability of $Ni_2Ti_4O$ using *ab-initio* total-energy calculations based on the local-density-functional scheme. The organization of the paper is as follows. In section 2, we briefly outline the method that we have used to solve the Schrödinger equation self-consistently. We show results for $Ni_2Ti_4O$ which is stabilized at a volume similar to those obtained for $NiTi_2$. In section 3, we study the electronic structure of the oxide $Ni_2Ti_4O$ and the site-projected energy analysis is also used to understand its stability. The discussion and conclusions are given in section 4.

## 2. Total-energy calculations

### *2.1. Structural information*

As mentioned in the introduction, $Ni_2Ti_4O$ has the same $E9_3$-type structure as $NiTi_2$ and the maximum oxygen solubility in the latter coincides with the filling of the 16d positions of space group $Fd3m$. Thus, the FCC unit cell for $Ni_2Ti_4O$ contains 112 atoms.

The positions of the metallic atoms in the unit cell correspond to three different Wyckoff positions, M(e), Ti(f) and Ti(c), defined as follows [5]:

$$48 \quad \text{Ti(f)} \quad x, 0, 0 \qquad 32 \quad \text{Ni(e)} \quad x', x', x' \qquad 16 \quad \text{Ti(c)} \quad \tfrac{1}{8}, \tfrac{1}{8}, \tfrac{1}{8}.$$

In the case of $NiTi_2$, $x = 0.311$ and $x' = 0.912$.

The structure can contain oxygen filling up an additional fourth Wyckoff position d, defined as follows:

$$16 \quad \text{O(d)} \quad \tfrac{5}{8}, \tfrac{5}{8}, \tfrac{5}{8}.$$

The intermetallic compound is thus transformed into the oxide $Ni_2Ti_4O$. The values of $x$ and $x'$ are slightly changed because of the presence of oxygen, i.e. $x = 0.312$ and $x' = 0.916$.

Their structure can be visualized as eight cubic subcells of two alternating patterns [5] as shown in figure 1, in which tetrahedra and octahedra are centred at the corners and centre of these small cubic cells. In order to show the internal arrangement of the subcells, the tetrahedra and octahedra shown in this figure have been collapsed about their centres. The subcell shown in figure 1($a$), present in $NiTi_2$ and $Ni_2Ti_4O$, has a large tetrahedron (titanium in the c positions) surrounding a smaller tetrahedron (nickel in the e positions) in the centre of this subcell. The other subcell shown in figure 1($b$) has a central octahedron (titanium in the f positions) for both $NiTi_2$ and $Ni_2Ti_4O$; however, in the case of $Ni_2Ti_4O$, a large tetrahedron (oxygen in the d positions) surrounds this central octahedron as shown. From investigation of the interatomic distances in $Ni_2Ti_4O$, the most important distinction from those of the $NiTi_2$ is that there are two oxygen atoms in the nearest neighbours for Ti(f) atoms with the relatively short distance Ti(f)–O (about 2.13 Å from experimental results) in comparison with other distances.

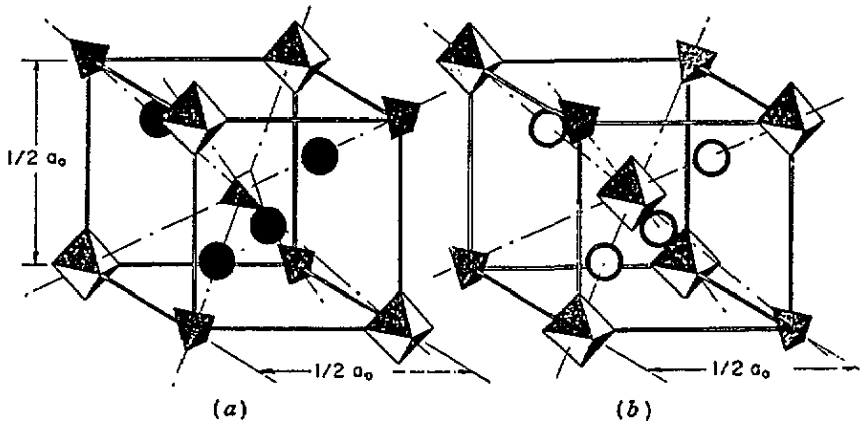


**Figure 1.** Schematic diagram showing the crystallographic subcell arrangement found in $Ni_2Ti_4O$ and $NiTi_2$: ●, 1 Ti(c) at $\frac{1}{8}, \frac{1}{8}, \frac{1}{8}$; ○, 1 O(d) at $\frac{5}{8}, \frac{5}{8}\frac{5}{8}$; ◇, 6 Ti(f) at $x, 0, 0$ ($x = 0.312$); △, 4 Ni(e) at $x', x', x'$ ($x' = 0.916$).

### *2.2. Method*

The total-energy studies are based on the local-density approximation (LDA) [6, 7], namely the self-consistent linear-muffin-tin-orbital (LMTO) method [8] and using two distinctly different approaches. In the first, the LMTOs are augmented with numerical solutions of the radial Schrödinger equation within non-overlapping muffin-tin spheres. No shape approximation for the potential or charge density is made. The output charge density and the product of two LMTOs (needed to construct the Hamiltonian matrix) are represented in the interstitial region by fitting a linear combination of Hankel functions to the values and slopes on the sphere boundaries [9]. The charge density is calculated exactly in the muffin-tin spheres in angular momentum components up to $l = 4$. We use the same angular momentum cut-off in the interpolation of quantities in the interstitial region, expanded in Hankel functions of energies $-1$ and $-3$ Ryd [9]. The interstitial exchange–correlation quantities are treated in the same way. This procedure makes it possible to evaluate the involved integrations over the interstitial region with little effort. In the second approach, we employ the atomic-spheres approximation (ASA) [10, 11] in which the spheres are permitted to overlap and are expanded until they fill the space. In addition, the so-called 'combined-correction term' [11] is included, which accounts for errors from overlapping spheres and from leaving regions not contained in any spheres.

For both approaches, the LMTO basis included s, p and d functions for each atom. The choice of the basis set that we found to be optimal for describing the valence band of the $NiTi_2$ and $Ni_2Ti_4O$ is $2s^22p^43d^0$ for oxygen, $4s^24p^03d^8$ for nickel and $4s^24p^03d^2$ for titanium. In order to provide sufficient variational freedom in the FP calculations, it is essential to employ LMTOs with various localizations in the calculation method that we used to extend the basis. The envelope function decays as $\exp(-\kappa r)$, where $-\kappa^2$ is the kinetic energy of the Hankel function envelope. For the first radial function, $\kappa_1^2 = -0.01$; for the second, $\kappa_2^2 = -1.0$; for the third, $\kappa_3^2 = -2.3$. The size of the secular matrix for FP calculations is then $616 \times 616$. Some FP calculations have also been performed, including $3p^6$ states of Ni and Ti. These 'semicore' electrons have been treated in the same way as the band states, by setting up and diagonalizing the Hamiltonian a second time. The effects of the 'two-panel calculations' in the final results (trends in the total energy as function of volume) has been

tested and found to be insignificant. With the basis set thus chosen, the FP calculated band structure is essentially insensitive to the particular choice of the muffin-tin sphere radii. We attempted to fill the space with spheres as densely as possible, but in such a way that the spheres never overlapped. We chose $r_{Ni} = 0.124a$, $r_{Ti} = 0.136a$ and $r_O = 0.083a$, leading to a space-filling factor of 55.2%. In the ASA, Wigner–Seitz radii are taken with the same ratio as given by the non-overlapping muffin-tin spheres.

The local-density potential of von Barth and Hedin [12] is used. To evaluate integrals over the Brillouin zone, we use a uniform mesh of sampling points which ensures that the total energy is converged to within 0.1 mRyd/atom. The $k$-integration is performed with the tetrahedron method with 29 irreducible $k$-points (i.e. 512 $k$-points in the Brillouin zone).

### 2.3. $Ni_2Ti_4O$

For both approaches, we have performed the self-consistent energy calculations as a function of volume. Figure 2 shows the calculated volume variation in the total energy by the FP LMTO method in order to locate the equilibrium lattice constant. We have found that the calculated lattice constant $a = 11.056$ Å is in good agreement with the experimental value ($a_{exp}(Ni_2Ti_4O) = 11.328$ Å [5]). This result is also in excellent agreement with our self-consistent ASA total-energy calculations that give $a = 11.162$ Å. From figure 2, we have calculated the bulk modulus directly from a numerical fit as proposed by Birch [13] and obtained the value of 1.856 Mbar for $Ni_2Ti_4O$.

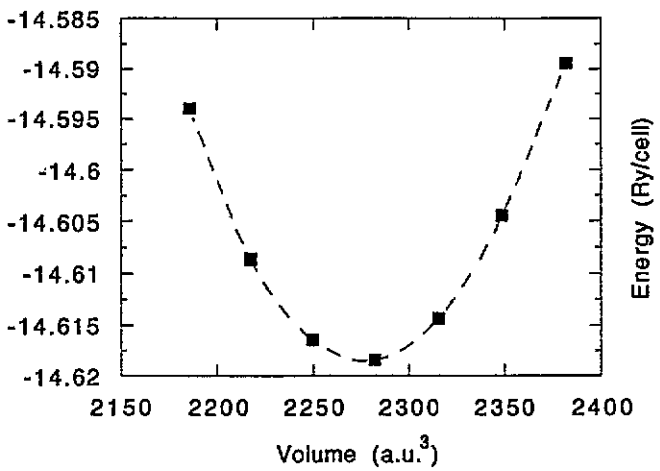


**Figure 2.** The scaled FP LMTO total-energy dependence for 28 atoms as a function of volume for the $Ni_2Ti_4O$ structure (a.u., arbitrary units).

## 3. Electronic structure and stability of the $Ni_2Ti_4O$ phase

### 3.1. Electronic structure

In order to understand the phase stability from the microscopic point of view, we inspect the electronic density of states (DOS) of $Ni_2Ti_4O$ and compare it with that obtained for $NiTi_2$ (cf figures 3 and 4). The total calculated DOS for both compounds are presented in figure 3. Except for the energy region lower than −0.4 Ryd, the band structures for $Ni_2Ti_4O$ and $NiTi_2$ are nearly similar; they originate essentially from Ni(3d)–Ti(3d) hybridization as

has been discussed in [3]. From the partial DOS analysis of $Ni_2Ti_4O$ (figure 4), the 3d hybridized states of Ni, Ti(f) and Ti(c) sites dominate the three principal peaks of the total DOS in the ranges from −0.3 to −0.1 Ryd, from −0.1 to 0.1 Ryd and from 0.1 to 0.3 Ryd, respectively. However, there is an important difference in this region between the two calculated DOS; the band structure and the Fermi level for $Ni_2Ti_4O$ are shifted to higher energies in comparison with those of $NiTi_2$. This behaviour is directly related to the formation of the oxygen hybridized band in the low-energy region between −0.7 and −0.4 Ryd. This band is separated from the above-discussed conduction band by a small gap of about 0.3 eV that can be observed in the total DOS of $Ni_2Ti_4O$. The global origin of these states, as may be seen from the partial DOS (figure 4), can be attributed to bonding hybridized O(2p)–Ti(f)(3d) states. This is coherent with the very small interatomic distance Ti(f)–O in $Ni_2Ti_4O$ as has been mentioned in section 2.

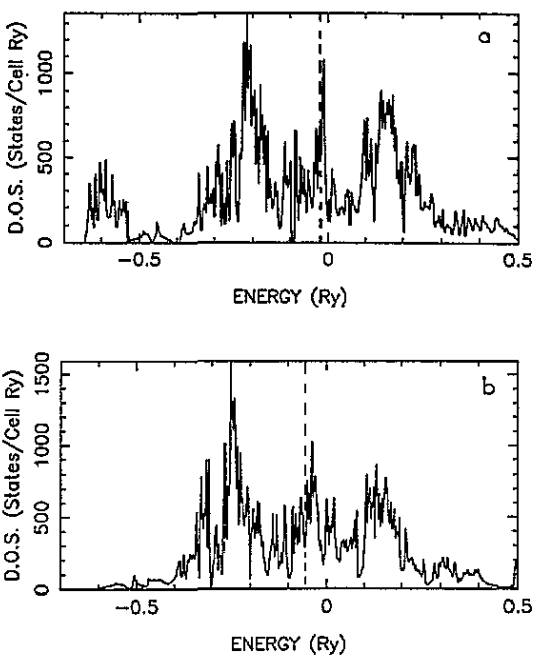


**Figure 3.** Total DOS for (*a*) the $Ni_2Ti_4O$ and (*b*) the $NiTi_2$ structures.

### *3.2. Site-projected energy analysis*

Using LMTO ASA calculations and a site-projected energy analysis [4] may also provide insight into the factors favouring the 'good' sites and the 'bad' sites in the structural energy calculations [14]. With a potential of the atomic sphere type and if the electronic density $n(r)$ is also approximated by the spherically averaged value, we obtain the following simple so-called ASA expression for the total energy per cell of the valence electrons and the ions:

$$E_{\text{tot}} = T_{\text{kin}} + \sum_R U_R + \sum_R \sum_{R'} Z_R Z_{R'} \sum_T |R - R' - T|^{-1} \tag{1}$$

where the first term is the kinetic energy, which should be expressed as the difference between the total energy and the potential energy of the non-interacting electrons. In the

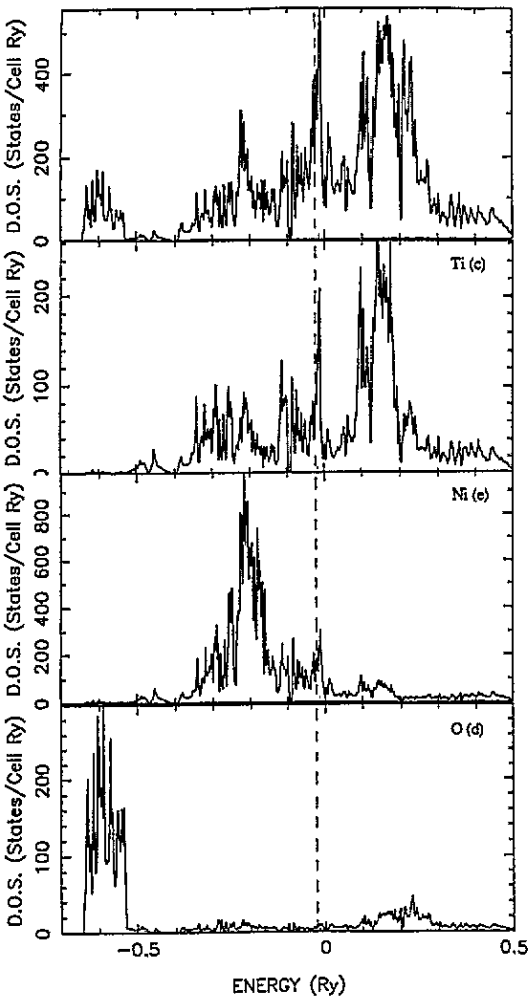


**Figure 4.** Partial DOS for $Ni_2Ti_4O$.

ASA, therefore,

$$T_{\text{kin}} = \int^{E_F} EN(E)\,\mathrm{d}E - \sum_R \int_0^{S_R} v_R(r) n_R(r) 4\pi r^2\,\mathrm{d}r = \sum_R T_R \qquad (2)$$

where $N(E) = \sum_{Rl} N_{Rl}(E)$ is the sum of the projected DOS, $v_R(r)$ is the one-electron potential in the sphere at $R$ and $n_R(r)$ is the spherically averaged charge density. The second term in equation (1) is the sum of the intra-sphere interactions between the electrons and the nucleons in that sphere. The third term is the inter-sphere Coulomb (or Madelung) energy. Here $z_R$ is the nuclear minus the electronic charge in the sphere at $R$. Equation (1) has thus proved useful for self-consistent calculations of the total site-projected energies in the cell and we use it in this work to investigate a local picture of the structural energies.

For $NiTi_2$, we have found that two types of Ti are favourable. However, the Ti(c) sites with an icosahedral environment (CN, 12) gain more energy in comparison with the Ti(f) sites (CN, 14). On the contrary, the Ni site is a 'bad' site in favouring the complex structure, since it has a more positive site-projected energy than that calculated in the corresponding pure Ni or in the two other structures ($MoPt_2$ type and $MoSi_2$ type). The same analysis

has been made for the oxide $Ni_2Ti_4O$ and the metallic projected-site energy calculations for both compounds are presented in table 1. Here one can conclude that the Ti(c) and Ti(f) sites display opposite roles in the two compounds considered; in the oxide, the Ti(f) sites gain more energy than Ti(c) sites. Thus, it seems that the introduction of oxygen into the intermetallic $NiTi_2$-type structure is an unfavourable factor for icosahedral formation.

**Table 1.** Site-projected energies of the three different types of atom in $Ni_2Ti_4O$ and $NiTi_2$, relative to the corresponding energies in pure metals.

| | $\Delta E$ (Ryd/atom) | |
|---|---|---|
| | $NiTi_2$ | $Ni_2Ti_4O$ |
| Ni | 0.141 54 | 0.088 49 |
| Ti(c) | −0.162 53 | −0.218 92 |
| Ti(f) | −0.095 64 | −0.424 28 |

## 4. Discussion and conclusions

In order to clarify the role of oxygen stability in the $NiTi_2$-type structure, we have used a tight-binding (TB) Hamiltonian which is directly analogous to the first-order LMTO Hamiltonian [15]:

$$H_{ij} = \bar{C}_i\delta_{ij} + \bar{\Delta}_i^{1/2}\bar{S}_{ij}\bar{\Delta}_j^{-1/2} \tag{3}$$

where $\bar{C}$ and $\bar{\Delta}$ are potential parameters in the TB representation and $\bar{\mathbf{S}}$ is the corresponding structure constant $\bar{C}_l$ determines the centre of the $l$-band while $\bar{\Delta}_l$ is related to its width. All these parameters are related to the orthogonal parameters $C_l$, $\Delta_l$ and $Q_l$ obtained from self-consistent LMTO ASA band-structure calculations by the following relations:

$$\frac{\bar{C}_l - E_l}{C_l - E_l} = \frac{\bar{\Delta}_l^{1/2}}{\Delta_l^{1/2}} = 1 - (Q_l - \bar{Q}_l)\frac{C_l - E_l}{\Delta_l}. \tag{4}$$

Here $\bar{Q}_l(= 0.3485, 0.053\,03, 0.010\,71)$ are the site-independent set of s, p, d screening constants in our LMTO equations. The calculated parameters $\bar{C}_l$ and $\bar{\Delta}_l$ for the two compounds $NiTi_2$ and $Ni_2Ti_4O$ are presented in tables 2 and 3, respectively. It is important to remember that the diagonal elements of the structure factor matrix $\bar{\mathbf{S}}_l$ do not vanish and they depend on the local environment. We have estimated these contributions to the one-site energies $\bar{C}_l$ and have found that they are negligible. The results in tables 2 and 3 may serve to construct the TB Hamiltonian for both structures considered and, for instance, some observations can be extracted from these tables.

(a) The p-site energy of oxygen is located at about −0.55 Ryd and it confirms the important contribution of O(2p) states in this energy region, as has been shown in section 3.

(b) The s- and d-site energies of TM sites for $Ni_2Ti_4O$ are shifted to higher energies in comparison with those obtained for $NiTi_2$, and this is coherent with the displacement of the electronic band structures observed in figure 3.

(c) The s, p contributions to the hopping energies of Ti(f) sites for $Ni_2Ti_4O$ decrease whereas its d contribution increases in comparison with the corresponding values for $NiTi_2$.

**Table 2.** TB Hamiltonian parameters of $NiTi_2$ deduced from the self-consistent LMTO potentials.

| | Ni | | Ti(c) | | Ti(f) | |
|---|---|---|---|---|---|---|
| | $\bar{C}_l$ | $\sqrt{\Delta_l}$ | $\bar{C}_l$ | $\sqrt{\Delta_l}$ | $\bar{C}_l$ | $\sqrt{\Delta_l}$ |
| 4s | −0.334 | 0.415 | −0.141 | 0.376 | −0.191 | 0.362 |
| 4p | 0.479 | 0.285 | 0.346 | 0.225 | 0.259 | 0.224 |
| 3d | −0.207 | 0.091 | 0.057 | 0.157 | 0.041 | 0.162 |

**Table 3.** TB Hamiltonian parameters of $Ni_2Ti_4O$ deduced from the self-consistent LMTO potentials.

| | Ni | | Ti(c) | | Ti(f) | | O(d) | |
|---|---|---|---|---|---|---|---|---|
| | $\bar{C}_l$ | $\sqrt{\Delta_l}$ | $\bar{C}_l$ | $\sqrt{\Delta_l}$ | $\bar{C}_l$ | $\sqrt{\Delta_l}$ | $\bar{C}_l$ | $\sqrt{\Delta_l}$ |
| 4s (2s for O) | −0.301 | 0.418 | −0.122 | 0.370 | −0.188 | 0.347 | −1.780 | 0.209 |
| 4p (2p for O) | 0.496 | 0.282 | 0.320 | 0.220 | 0.135 | 0.192 | −0.550 | 0.182 |
| 3d | −0.161 | 0.104 | 0.083 | 0.173 | 0.053 | 0.174 | 3.201 | 0.214 |

This behaviour shows that the hybridization between 3d(Ti(f))–2p(O) states is responsible for the modifications of the 3d–TM band and it appears as a peculiar property of the chemical bonding interaction in $Ni_2Ti_4O$.

In conclusion, we have studied the stability of the oxide $Ni_2Ti_4O$ by means of FP calculations. The DOS calculations combined with the site-projected energy analysis allow us to show that, in $Ni_2Ti_4O$, the Ti(f) site with non-icosahedral symmetry is the favoured site for stabilization, because of the effects of the 2p(O)–3d(Ti(f)) hybridization. The LMTO TB parameter calculations serves to confirm the coherent interpretation of our results.

## Acknowledgments

D Nguyen Manh would like to thank LTPCM for its invitation and financial support.

## References

[1] *Watson* R E and Bennett L H 1984 *Acta Metall.* 32 477
[2] Nevitt M V 1960 *Trans. Metall. Soc. AIME* 218 327
[3] Nguyen Manh D, Pasturel A, Paxton A T and van Schilfgaarde M 1993 *Phys. Rev.* B 48 14 801
[4] Nguyen Manh D, Pasturel A, Paxton A T and van Schilfgaarde M 1993 *J. Phys.: Condens. Matter* 5 9087
[5] Mueller M H and Knott H W 1963 *Trans. Metall. Soc. AIME* 227 674
[6] Hohenberg P C and Kohn W 1964 *Phys. Rev.* 136 B864
[7] Kohn W and Sham L J 1965 *Phys. Rev.* 140 A1133
[8] Andersen O K 1975 *Phys. Rev.* B 12 3060
[9] Methfessel M 1988 *Phys. Rev.* B 38 1537
[10] Andersen O K 1973 *Solid State Commun.* 13 133
[11] Andersen O K 1984 *Electronic Structure of Complex Systems* ed P Phariseau and W M Temmerman (New York: Plenum) p 11
[12] von Barth U and Hedin L 1972 *J. Phys. C: Solid State Phys.* 5 1629
[13] Birch F 1978 *J. Geophys. Res.* 83 1257
[14] Phillips R, Deng H, Carlsson A E and Daw M S 1991 *Phys. Rev. Lett.* 67 3128
[15] Andersen O K and Jepsen O 1984 *Phys. Rev. Lett.* 53 2571